

$\text{Nd}_1 + \epsilon\text{Fe}_4\text{B}_4$, a novel system of infinitely adaptive structures

This article has been downloaded from IOPscience. Please scroll down to see the full text article.

1989 J. Phys.: Condens. Matter 1 7513

(<http://iopscience.iop.org/0953-8984/1/41/001>)

View [the table of contents for this issue](#), or go to the [journal homepage](#) for more

Download details:

IP Address: 171.66.16.96

The article was downloaded on 10/05/2010 at 20:27

Please note that [terms and conditions apply](#).

Nd₁ + εFe₄B₄, a novel system of infinitely adaptive structures

Z B Zhao[†], S K Xia[†], C R Wang[‡] and R Z Ma[†]

[†] Department of Materials Physics, Beijing University of Science and Technology, Beijing 100083, People's Republic of China

[‡] Department of Surface Science and Corrosion Engineering, Beijing University of Science and Technology, Beijing 100083, People's Republic of China

Received 3 February 1989

Abstract. The Nd₁ + εFe₄B₄ compound, built up by the interpenetration of two mutually incommensurate substructures, presents a novel example of Vernier structure or chimney-ladder structure. This compound has been investigated by means of x-ray diffraction, electron diffraction and electron microscopy. The results indicate that the Nd₁ + εFe₄B₄ compound exhibits the characteristics of infinitely adaptive structures. Several different superstructures, at least on the microscopic scale, have been observed. It is suggested that the structure adaptability in this system is realised due to the displacive flexibility of one-dimensional Nd atom chains along the *c* direction.

Since the outstanding magnetic properties of Nd–Fe–B were discovered, the identified minor phase Nd₁ + εFe₄B₄ (ε ≃ 0.1), also called the boron-rich phase, has been subject to several investigations (e.g. Bezinge *et al* 1985, Givord *et al* 1985, 1986a, b, c, Niarchos *et al* 1986). In particular, most efforts have been devoted to its unique structural aspect. As first proposed by Braun *et al* (1982), this compound is built up by the interpenetration of two mutually incommensurate substructures, i.e. Fe–B substructure and Nd substructure. A similar structural build-up principle can also apply to the other R₁ + εFe₄B₄ (R represents rare earth elements) compounds (e.g. Bezinge *et al* 1985). The general structural feature of the Nd₁ + εFe₄B₄ compound has been revealed by Givord *et al* (1985, 1986a, b). In this compound, the framework of three-dimensionally linked edge-sharing tetrahedra of Fe atoms, strongly coupling with dumbbells of B atoms, forms the Fe–B substructure; on the other hand the infinite Nd–Nd chains, parallel to the *c* axis, spacing in the octogon channels of the former substructure, constitute the Nd substructure. Two substructures both belonging to the tetragonal system share the same lattice dimensions in the tetragonal basal plane. However, of particular interest is that their periods in the *c* direction do not match. Accordingly the *c* uniaxial periodicity of this compound has to be characterised simultaneously by two translation vectors *c*(Fe–B) and *c*(Nd), and the Nd₁ + εFe₄B₄ compound forms the Vernier structure or chimney-ladder structure. It was found that in the MnSi_{2–x} related system of the Nowotny phase (e.g. Knott *et al* 1967, de Ridder *et al* 1976, Ye and Amelinckx 1986) and Ba₁ + xFe₂S₄ (e.g. Grey 1974, 1975) a similar structural principle applies.

In order to examine structure variation of the Nd₁ + εFe₄B₄ compound with the composition, several samples with different nominal compositions were investigated by

Table 1. The lattice parameters of the $\text{Nd}_1 + \varepsilon\text{Fe}_4\text{B}_4$ compound for the cases of different nominal composition x in $\text{Nd}_x\text{Fe}_4\text{B}_4$ samples. The numbers in parentheses are the estimated deviations for the last significant figure.

x	0.8	0.9	1.0	1.1	1.2	1.3	1.4	1.5
a (nm)	0.7117(1)	0.7122(1)	0.7124(1)	0.7109(1)	0.7114(2)	0.7109(3)	0.7116(1)	0.7119(5)
$c_{\text{Fe-B}}$ (nm)	0.3891(1)	0.3893(1)	0.3896(1)	0.3892(3)	0.3894(1)	0.3893(2)	0.3900(1)	0.3888(4)
c_{Nd} (nm)	0.3559(2)	0.3546(3)	0.3513(2)	0.3505(3)	0.3496(4)	0.3482(6)	0.3466(1)	0.3446(5)
$1 + \varepsilon$	1.093	1.098	1.109	1.110	1.114	1.118	1.125	1.128

x-ray diffraction. As the ratio $c(\text{Fe-B})/c(\text{Nd})$ can hardly be represented by two relatively small integers, the $\text{Nd}_1 + \varepsilon\text{Fe}_4\text{B}_4$ compound forms either the incommensurate structures, or the commensurate superstructures with unusual long period in the c direction. Unfortunately the resolution of the presently available x-ray diffraction data fails to give an unambiguous judgement on this point; also the results of electron diffraction on such compounds have been little reported so far. One purpose of this paper is to reveal by electron microscopy further structural aspects of the $\text{Nd}_1 + \varepsilon\text{Fe}_4\text{B}_4$ compound.

The alloys with nominal composition $\text{Nd}_x\text{Fe}_4\text{B}_4$ ($x = 0.8, 0.9, \dots, 1.5$) have been produced by vacuum arc melting of high-purity constituents. For homogenisation, the obtained ingots were sealed in evacuated quartz tubes, and annealed at 1300 K for 40 days. The powder specimen of each bulk sample was examined on a Rigaku diffractometer using monochromated $\text{Cu K}\alpha$ radiation. The lattice parameters were fitted by the least-squares method. In order to prepare the specimen for observation on TEM, the ingots were crushed into rather fine fragments, then dispersed in ethyl alcohol and collected on carbon-coated, perforated plastic films supported by copper meshes of 3 mm in diameter. The properly selected fragments were observed on an H-800 electron microscope at the accelerating voltage 200 KV.

The x-ray diffraction results indicate that in each bulk sample the $\text{Nd}_1 + \varepsilon\text{Fe}_4\text{B}_4$ compound serves as the main phase in equilibrium with other impurity phases. For the sake of convenience, the samples are labelled by their nominal compositions x , although the actual compositions of the samples deviate from x owing to loss during melting. The powder x-ray diffraction patterns for the $\text{Nd}_1 + \varepsilon\text{Fe}_4\text{B}_4$ compound consist of two sets of relatively strong reflections which can be attributed to either Fe-B substructure, or Nd substructure, or the common contribution of these two substructures. For the samples with different nominal compositions, the corresponding x-ray diffraction patterns of the $\text{Nd}_1 + \varepsilon\text{Fe}_4\text{B}_4$ compound show little difference apart from the small position shift of certain reflections. The fitted lattice parameters, under the acceptance of tetragonal symmetry and the coexistence of dual periods, are presented in table 1. It can be seen that the dimensions in the tetragonal basal plane and $c(\text{Fe-B})$ all exhibit little variation as the nominal composition x changes. However, $c(\text{Nd})$ which ranges from 0.3559 to 0.3446 nm shows a relatively strong dependence on x . According to the atomic arrangement in the crystal structure of $\text{Nd}_1 + \varepsilon\text{Fe}_4\text{B}_4$, refined by Givord *et al* (1985, 1986a, b) and Bezingé *et al* (1985), its composition ε can only be related to the ratio of two periods in the c axis, i.e. $1 + \varepsilon = c(\text{Fe-B})/c(\text{Nd})$. It follows from this relation that the $\text{Nd}_1 + \varepsilon\text{Fe}_4\text{B}_4$ compound spans a homogeneity range of $0.093 < \varepsilon < 0.128$ as indicated in table 1. Of great interest is that such a variation of composition attains through the change of $c(\text{Nd})$ as a function of x in $\text{Nd}_x\text{Fe}_4\text{B}_4$ rather than the usual way of solid solution (either substitutional or interstitial). Such structural feature can be characterised by 'infinitely adaptive structures'. This terminology was proposed by

Anderson (1973, 1977) to describe certain crystalline systems in which 'within certain composition limits, every possible composition can attain a unique, fully ordered structure, without defects arising from solid solution effects and with no biphasic coexistence ranges between successive structures', but to date such systems have not often been well recognised (Cheetham 1981). For a given value of the ratio $c(\text{Fe-B})/c(\text{Nd})$, one can, of course, always find two integers p and q , with a specified tolerance, to meet the need of $p/q = c(\text{Fe-B})/c(\text{Nd})$. Thus high-order commensurate models $\text{Nd}_p(\text{Fe}_4\text{B}_4)_q$ can be constructed. $\text{Sm}_{17}(\text{Fe}_4\text{B}_4)_{15}$ and $\text{Nd}_{10}(\text{Fe}_4\text{B}_4)_9$, for example, are selected by Bezinge *et al* (1985) and Givord *et al* (1985, 1986a, b) in structure refinements.

As argued by Anderson (1977), the adaptive structure presents a way in which long-period modulation can be impressed on the basic lattice. However, in powder x-ray diffraction patterns of the $\text{Nd}_1 + \varepsilon\text{Fe}_4\text{B}_4$ compound, only several reflections attributed to the basic lattice of Fe-B substructure and Nd substructure appear; no satellite reflections corresponding to superlattice structure can be observed. Such deficiency is expected to be overcome by electron diffraction and electron microscopy.

To understand the observed electron diffraction patterns (hereafter denoted by EDP), we first discuss the predicted EDP based on the general structural feature of the $\text{Nd}_1 + \varepsilon\text{Fe}_4\text{B}_4$ compound. Since period mismatching happens only in the c axis, the most typical and useful EDP should be $(UV0)^*$ sections. Taking the extinction rules arising from the space groups $P4_2/nm$ of the Fe-B substructure and $I4/mmm$ of the Nd substructure (Givord *et al* 1985) into account, we expect patterns composed of just the basic reflections as in figures 1(a) and 1(c). Such patterns, although not really existing but nevertheless playing an important role in characterising the general feature of EDP of the $\text{Nd}_1 + \varepsilon\text{Fe}_4\text{B}_4$ compound, are defined as the basic patterns. Here the notation of four indices (hkl_1l_2) is adopted in view of the coexistence of two incommensurable sublattices. (hkl_1l_2) represents the basic reflections of the Nd substructure for $l_1 = 0$, those of the Fe-B substructure for $l_2 = 0$, and those contributed commonly by the two substructures when $l_1 = l_2 = 0$. Apparently, the basic patterns only present the idealised case of a Vernier structure which is interpenetrated by two undistorted substructures. As a matter of fact, two substructures would interact with each other rather than be completely independent. Therefore satellite reflections should arise. The periodicity (if any) of the coupled superstructure determines the distribution of the satellites whose extinction rules are determined by the symmetry of the selected $\text{Nd}_p(\text{Fe}_4\text{B}_4)_q$ model. Thus the qualitative EDP (i.e. without considering the intensity) of commensurate models $\text{Nd}_{10}(\text{Fe}_4\text{B}_4)_9$ (space group $Pccn$, Givord *et al* 1985) with $c = 10c(\text{Nd}) = 9c(\text{Fe-B})$ and $\text{Nd}_9(\text{Fe}_4\text{B}_4)_8$ (space group $Ccca+$) with $c = 9c(\text{Nd}) = 8c(\text{Fe-B})$, for instance, are illustrated in figures 1(b) and 1(d), respectively. They are, qualitatively, in agreement with the observed EDP shown in figure 2, which confirms in the $\text{Nd}_1 + \varepsilon\text{Fe}_4\text{B}_4$ compound the structural build-up principle of the Vernier structure. From several representative observed EDP in figure 2, one can see that the satellites whose corresponding positions are indicated by arrows in figure 1(b) and 1(d) exhibit the unexpected strong intensity; also the $(00l_1l_2)$ rows in $(100)^*$ patterns show different characteristics from those in $(\bar{1}10)^*$ patterns. It was found that such phenomena are attributed to the dynamical effect of electron diffraction. Seen from figure 2, the diffraction vectors of the reflections in the observed EDP can be represented, according to the Vernier model, by $\mathbf{G} + 2m\mathbf{g}$, where \mathbf{G} represents the reciprocal vector of either the Fe-B or Nd sublattices and $|\mathbf{g}|$ is equal to $1/c(\text{Nd}) - 1/c(\text{Fe-B})$. Although clearly showing similarities for the same zone patterns, the EDP with differently distributed satellites are identified by scrutiny. The illustration for each long-period superstructure is presented by the onsets, with the

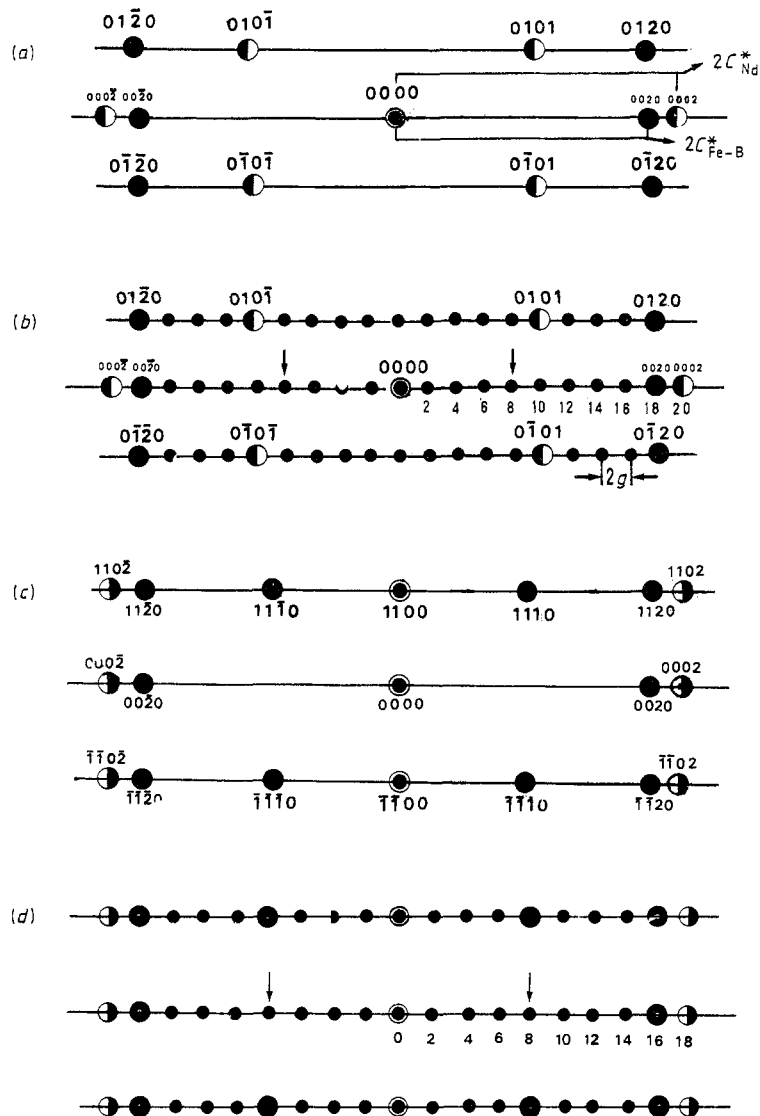


Figure 1. Illustration of the predicted EDP of the $\text{Nd}_1 + e\text{Fe}_4\text{B}_4$ compound, visualised according to the Vernier structure model. Parts (a) and (c) present the basic patterns of $(100)^*$ and $(\bar{1}10)^*$, respectively. Under the commensurate models, the qualitative EDP $(100)^*$ of $\text{Nd}_{10}(\text{Fe}_4\text{B}_4)_9$ (b) and $(\bar{1}10)^*$ of $\text{Nd}_9(\text{Fe}_4\text{B}_4)_8$ (d) can be obtained. The arrows indicate that the observed satellites corresponding to these positions exhibit the unexpected strong intensity due to the double diffraction. ● indicates the basic reflection of the Fe-B substructure; ○ the basic reflection of the Nd substructure; ⊙ the reflection commonly contributed by Fe-B and Nd substructures; • the satellite reflection.

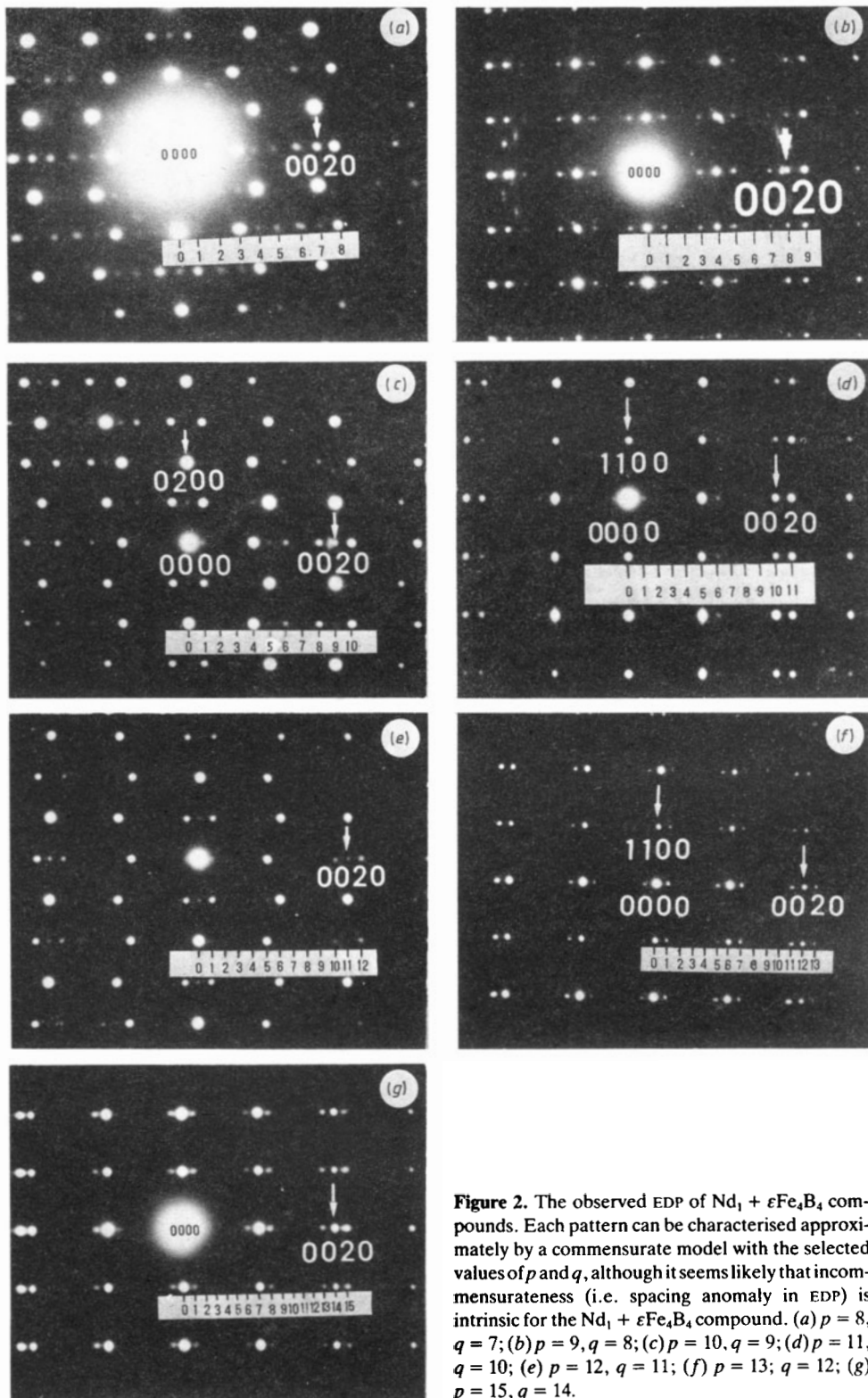


Figure 2. The observed EDP of $Nd_1 + \epsilon Fe_4B_4$ compounds. Each pattern can be characterised approximately by a commensurate model with the selected values of p and q , although it seems likely that incommensurateness (i.e. spacing anomaly in EDP) is intrinsic for the $Nd_1 + \epsilon Fe_4B_4$ compound. (a) $p = 8$, $q = 7$; (b) $p = 9$, $q = 8$; (c) $p = 10$, $q = 9$; (d) $p = 11$, $q = 10$; (e) $p = 12$, $q = 11$; (f) $p = 13$; $q = 12$; (g) $p = 15$, $q = 14$.

opposite contrast, in figure 2(a-g). In terms of the commensurate models, each satellite is rationalised to the rational numbers which are determined by the selected value of p and q . Because of the close spacing of the satellites, it is difficult to obtain more exact p and q . However, the commensurate model we choose here is merely used to characterise the differences among the EDP; the accurate values of p and q are unimportant in this respect. In fact, only typical examples of EDP which are near to the commensurate models are presented in figure 2. The positions of satellites seems to exhibit the quasicontinuous drift within a certain range and the spacing anomaly arises, i.e. there is no smallest common multiple of $c(\text{Fe-B})$ and $c(\text{Nd})$. One can see, for instance, that in figure 2(a) the satellite labelled 6 is not exactly halfway between the satellites labelled 5 and 7. Also in view of the frequent occurrence of the orientation anomaly (Zhao *et al* 1989), it seems likely that the incommensurateness is the intrinsic structural feature for the $\text{Nd}_1 + \epsilon\text{Fe}_4\text{B}_4$ compound. In the terminology of Janner *et al* (1980) and Janssen *et al* (1987), such systems which are composed of two or more incommensurate subsystems are called incommensurate composite structures.

No unique relationship between the EDP of the $\text{Nd}_1 + \epsilon\text{Fe}_4\text{B}_4$ compound and the nominal compositions x in $\text{Nd}_x\text{Fe}_4\text{B}_4$ can be observed. Occasionally, the same-zone EDP with different characteristics can also be obtained in the same bulk samples. Accurately speaking, the bulk samples are microscopically inhomogeneous, even after long-period (40 days) annealing treatment. The x-ray diffraction results in table 1 can be considered as those of a statistically averaged Vernier structure.

The structure adaptability of the $\text{Nd}_1 + \epsilon\text{Fe}_4\text{B}_4$ compound can also be reflected by the fringe images (g -fringe) corresponding to $2g$ vectors indicated in figure 1(b). As shown in figures 3(a) and 3(b), the interspacing of fringe images can be related to the periods of two substructures, namely equal to $c(\text{Fe-B})c(\text{Nd})/(c(\text{Fe-B})-c(\text{Nd}))$. The nature of such fringe contrast has not yet been well understood. In the incommensurate composite systems, the modulation owing to the interaction between the subsystems has been both observed experimentally (e.g. Johnson and Watson 1976, Currat 1984) and considered theoretically (e.g. see Theodorou and Rice 1978, Axe and Bak 1982). We suggest that the fringes imaged by the $2g$ vector are perhaps the modulation-wave-related contrast. As the periods of two substructures, particularly $c(\text{Nd})$, change as a function of composition, a variation of interspacing in fringe images is expected. Such a variation can be observed by two examples in figure 3. In most cases, the fringe images are not as perfect as in figure 3(a). The imperfection of the fringe images, e.g. in figure 3(b), may be indicative of further structural details such as the local existence of composition fluctuation or misaligned interpenetration of two substructures. However, the accumulated experimental evidence is insufficient to open this argument.

As mentioned above, the $\text{Nd}_1 + \epsilon\text{Fe}_4\text{B}_4$ compound can couple to various different superstructures, without apparent destruction of long-range ordering, in response to the composition variation. According to the results of Givord *et al* (1985, 1986a, b), Fe-B distances on average are 15% shorter than the sum of their atomic radii. This fact suggests the rather strong interaction between Fe and B atoms. Therefore the framework of the Fe-B substructure is of remarkable rigidity and shows almost independence of the nominal composition x . It can be concluded that the structure adaptability attains chiefly due to the elongating or shrinking of the repeat length of one-dimensional Nd atom chains. The relatively wide variation range of $c(\text{Nd})$ (see table 1) requires the displacive flexibility of Nd atoms along the c direction. The atomic vibration factors of $\text{R}_1 + \epsilon\text{Fe}_4\text{B}_4$ compounds have not been given in the structure refinements of Givord *et al* (1985, 1986a, b) and Bezinge *et al* (1985). However, many RT_4B_4 compounds (T

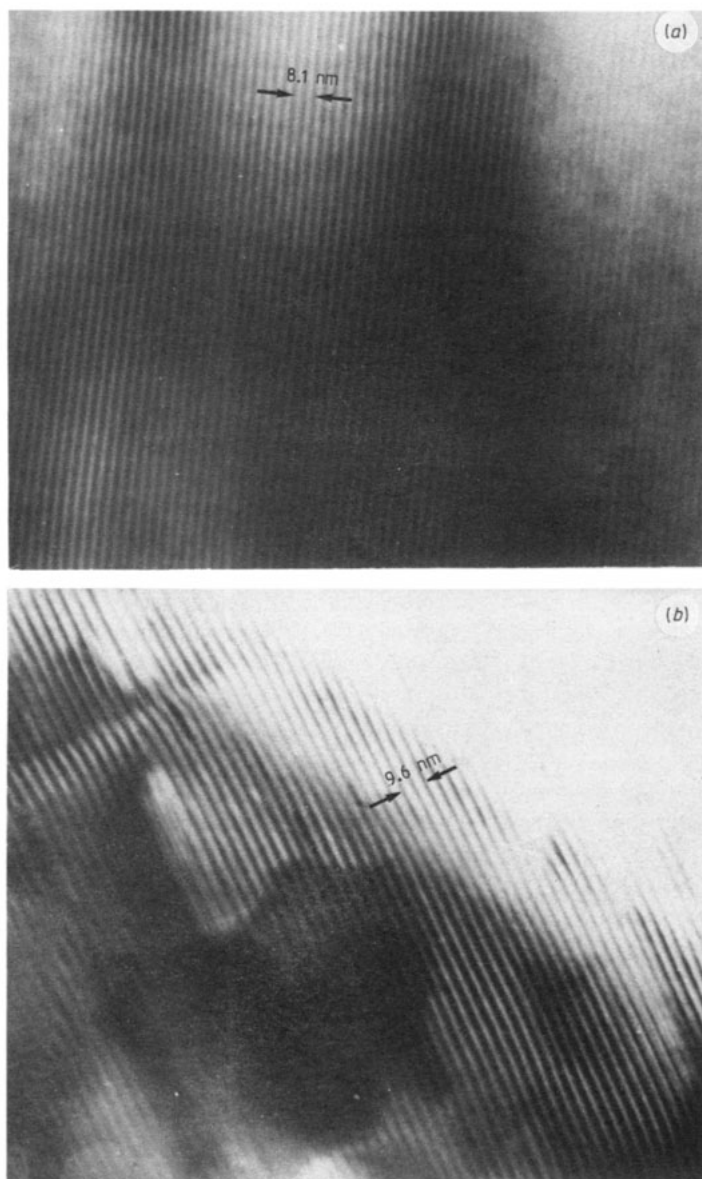


Figure 3. Two *g*-fringe images with different interspacings of the $Nd_1 + \epsilon Fe_4B_4$ compound. In the case of (b), the fringe image is not as perfect as in (a) and the locally-bent area exhibits a dislocation-like configuration.

represents the transition elements) with the $NdCo_4B_4$ structure type have very similar atomic linkage and, simply, the period of the R substructure agrees with that of the T-B substructure. In such a kind of tetraboride, the vibration factors of rare earth atoms often show an extremely large component in the *c* direction (e.g. Hiebl *et al* 1981, Rogl 1980). Thus it seems likely that the structure adaptability is realised owing to the displacive flexibility of the Nd atoms.

In conclusion, it is worthwhile to mention, in view of its unique structural feature, that the $Nd_1 + \epsilon Fe_4B_4$ compound may be expected to serve as an incommensurate system which can be described by the devil's staircase (Bak 1982).

Acknowledgments

The authors gratefully acknowledge Dr B H Miao of the Electron Microscopic Laboratory at BUST for his kind help. One of us, Z B Zhao, also wishes to express his thanks to Professor H S Xie at the Geochemical Research Institute, Academia Sinica, and Dr R L Withers at the Research School of Chemistry, Canberra, for stimulating discussions.

Note added. It can be derived, based on the argument of Buerger (1947) about the symmetry of derivative crystal structure, that the space group symmetry of the commensurate model $\text{Nd}_p(\text{Fe}_4\text{B}_4)_q$ is dependent on the parity combination of p and q , and in case of p odd and q even the highest symmetry of $\text{Nd}_p(\text{Fe}_4\text{B}_4)_q$ should be $Ccca$ in the revised supercell with translation vectors $A = a + b$, $B = b - a$ and $C = c$.

References

- Anderson J S 1973 *J. Chem. Soc. Dalton Trans.* 1107
 ——— 1977 *J. Physique* **C7** 17
 Axe J D and Bak P 1982 *Phys. Rev. B* **26** 4963
 Bak P 1982 *Rep. Prog. Phys.* **45** 587
 Bezinge A, Braun H F, Muller J and Yvon K 1985 *Solid State Commun.* **55** 131
 Braun H F, Pelizzone M and Yvon K 1982 *Proc. 7th Int. Conf. Solid Compounds of Transition Elements, Grenoble part II B*, p11
 Buerger M J 1947 *J. Chem. Phys.* **15** 1
 Cheetham A K 1981 *Nonstoichiometric Oxides* (New York: Academic) p 426
 Currat R 1984 *Modulated Structure Materials* (Dordrecht: Nijhoff) p 285
 De Ridder R, Van Tendeloo G and Amelinckx S 1976 *Phys. Stat. Sol.* **33** 383
 Givord D, Moreau J M and Tenaud P 1985 *Solid State Commun.* **55** 303
 Givord D, Tenaud P and Moreau J M 1986a *J. Less-Common Metals* **115** L7
 ——— 1986b *J. Less-Common Metals* **123** 109
 ——— 1986c *J. Magn. Magn. Mater.* **54–57** 445
 Grey I E 1974 *J. Solid State Chem.* **11** 128
 ——— 1975 *Acta Crystallogr. B* **31** 45
 Hiebl K, Sienko M J and Rogl P 1981 *J. Less-Common Metals* **82** 21
 Janner A and Janssen T 1980 *Acta Crystallogr. A* **36** 408
 Janssen T and Janner A 1987 *Adv. Phys.* **36** 519
 Johnson C K and Watson Jr C R 1976 *J. Chem. Phys.* **64** 2271
 Knott H W, Mueller M H and Heaton L 1967 *Acta Crystallogr.* **23** 549
 Niarchos D, Zouganelis G, Kostikas A and Simopoulos A 1986 *Solid State Commun.* **59** 389
 Rogl P 1980 *Mh. Chem.* **111** 517
 Theodorou G and Rice T M 1978 *Phys. Rev. B* **18** 2840
 Zhao Z B, Xia S K, Ma R Z, Ping J Y, Miao B H and Pan S M 1989 *Solid State Commun.* **69** 1011
 Ye H Q and Amelinckx S 1986 *J. Solid State Chem.* **61** 8